Research papers

Applicability of Diffusive model for mud-flows: An unsteady analysis

Cristiana Di Cristo [a],[*], Michele Iervolino [b], Tommaso Moramarco [c], Andrea Vacca [a]

[a] Dipartimento di Ingegneria Civile, Edile ed Ambientale, Università degli Studi di Napoli "Federico II", Via Claudio 21, 80125 Napoli, Italy
[b] Dipartimento di Ingegneria, Università degli Studi della Campania "Luigi Vanvitelli", Via Roma 29, 81031 Aversa, CE, Italy
[c] National Research Council, IRPI, Via Madonna Alta 126, Perugia, Italy

ARTICLE INFO

ABSTRACT

Simplified versions of the Shallow Water Equations, known as Kinematic and Diffusive models, are commonly applied to the analysis of debris- and mud- flow dynamics. For this reason, the study of their applicability conditions represents an important concern. The present work investigates on the applicability conditions of the Diffusive Wave Model (DWM) for the prediction of mud-flows of shear-thinning fluid represented by a power-law rheology. The study has been carried out through the numerical solution of the DWM and the Full Wave Model (FWM) in unsteady conditions with hydrographs of different durations assigned at the channel inlet. The analysis has considered different rheological indexes, several values of the Froude (F) and of the Kinematic Wave (K) numbers. Predictions of DWM and FDM have been compared considering the mean value of dimensionless errors on maximum flow depth, ε_h^*, and maximum discharge ε_q^*. Positive (negative) error leads to an overestimation (underestimation) of the maximum flow depth and flow discharge in the prediction of the DWM. In the present analysis the DWM is considered safely applicable in case of underestimation, i.e. for positive values of ε_h^* and ε_q^*. Negative errors are acceptable if their absolute value is smaller than 5%. For all the investigated values of the governing parameters, the performance of the DWM has been found to strongly depend on the value of the rheological index, worsening as the fluid rheology becomes more shear-thinning. Regardless of the hydrograph duration, and for fixed power-law exponent (n) and F values, results indicate the existence of limiting values of the kinematic wave number $\overline{K}_h$ and $\overline{K}_q$ above which the DWM is applicable in terms of maximum depth and discharge, respectively. For K values smaller than $\overline{K}_h$ and $\overline{K}_q$, the DWM applicability depends also on the hydrograph duration. In these conditions and for several values of the (F, n) pair, the threshold values of the hydrograph duration necessary for DWM applicability have been identified. The presented applicability criteria represent a useful guideline for the practical application of the DWM in assessing the hazard of a mud flood.

1. Introduction

Debris- and mud-flows involve fast-moving mixtures of water with great volumes of sediment. Typically, they develop in mountain areas triggered by heavy rains (Hutter et al., 1994; Iverson and Denlinger, 2001) particularly after wildfires (Rengers et al., 2016), since they reduce the surface water storage (Benavides-Solorio and MacDonald 2005) and promote the infiltration of the rain decreasing the canopy interception (Stoof et al., 2012). Debris- and mud- flows may produce huge damages and loss of lives (Hurlimann et al., 2006; Di et al., 2008) and cause dramatic changes of the topography, the river morphology (Brown and Pasternack 2014), and even the coastal areas (Ciervo et al., 2015). Owing to their destructive power, these flows have high socio-

economic impacts (Fuchs et al., 2007; Thiene et al., 2017) and therefore the definition of appropriate mathematical models for predicting their impact is crucial. The selection of the most adequate model for the debris- and mud-flows analysis implies a choice among many available options. A first approach assumes a single-phase description of the flowing medium considered as a homogeneous continuum with a non-Newtonian behavior. However, the use of a constant rheology does not furnish accurate predictions for debris-flows when temporal and spatial variations of the pore fluid pressure and mixture agitation occur, or when mixture composition changes due to segregation of solid particles (Iverson 2003). Alternative approaches are represented by quasi-single phase mixture (e.g. Xia et al., 2018) and two-phase (e.g. Iverson, 1997; Pitman and Le, 2005; Di Cristo et al., 2016; Li et al., 2018a,

2018b) models. For instance, Iverson (1997) and Iverson and Denlinger (2001) proposed a Coulomb mixture theory for debris-flows which considers the interaction between the fluid phase, assumed as a Newtonian fluid, and the granular solid, which behaves as a Coulomb fictional material. Greco et al. (2019) compared the performance of two different depth-integrated theoretical models, Single-Phase Model (SPM) and Two-Phase Model (TPM), in reproducing the impact of a mud-flow on rigid obstacles to evaluate the force acting on them. The two models show comparable results for the considered two-dimensional test case, while some differences are observed in simulating a 1D landslide over a very steep slope.

In the framework of the single-phase models different formulations have been proposed. Some of them assume the existence of a yield stress, such as Bingham (Liu and Mei, 1989; Imran et al., 2001; Hewitt and Balmforth, 2013) and Herschel–Bulkley (Coussot, 1997; Huang and Garcia, 1998; Chanson et al., 2006) models. Conversely, the power-law model, without the yield stress, is often adopted for mud-flows, characterized by mixtures of fine sediment and water, with a rheology strongly influenced by the quantity of the fine fraction. In particular, the shear-thinning power-law model, characterized by an exponent lower than one, is particularly adequate for flows with a finite fraction of coarse grains (Ng and Mei, 1994; Hwang et al., 1994; Perazzo and Gratton, 2004; Longo et al., 2015), encountered for instance in natural estuaries (Zhang et al., 2010) or during landslides (Carotenuto et al., 2015). The power-law model may also result preferable when the correct rheological characterization of a visco-plastic fluid appears difficult (Ovarlez et al., 2011; Chambon et al., 2014).

Although in several cases three-dimensional effects are not negligible, depth-averaged models based on 2D shallow-water equation (SWEs) are widely accepted for many engineering applications (Iverson and George, 2014; Fent et al., 2018) such as for mud-flows routing (Armanini et al., 2014; Rosatti and Begnudelli, 2013; Di Cristo et al., 2020).

Moreover, even though efficient numerical methods for the solution of the SWEs are currently available, simplified models, derived neglecting one or more terms in the momentum equation are often used. Among the approximate models, we cite the widespread Kinematic Wave Model (KWM) and Diffusive Wave Model (DWM). In particular, the DWM is usefully applied in flood modelling and rainfall-runoff simulations (Aricò et al., 2011; Caviedes-Voullieme et al., 2020), but also coupled with sewage models (Martins et al., 2017). In particular, Prestinizi (2008) tested the DWM for reproducing a dam-break denoting that it is able to reproduce the principal features of the inundation.

As far as non-Newtonian fluids are concerned, the comparison between the numerical results and laboratory experiments, carried out with reference to Bingham (e.g. Liu and Mei 1989), Herschel–Bulkley (e. g. Ancey et al., 2012) and power-law (e.g. Longo et al., 2015) fluids, suggests that the DWM may describe the essential features of a mud-flow wave. In particular, Longo et al. (2015) analysed the performance of both Kinematic and Diffusive models in reproducing the laboratory experiments concerning the propagation of a power-law fluid wave in channels. Theoretical solutions are obtained for inclined channel in self-similar form for the DWM and with the method of characteristics for the KWM. It has been shown that the theoretical solutions describe with sufficient accuracy the front propagation before the transition to longer roll-waves. Simplified models have been successfully applied also for reproducing the dynamics of debris- and mud-flows (O'Brien et al., 1993; Arattano and Franzi, 2010; Chiang et al., 2012; Gregoretti et al., 2016, 2019; Bernard et al., 2019).

In clear-water turbulent flows, the applicability conditions of both Kinematic and Diffusive models have been deeply studied either analysing their linearized version (Tsai 2003) or accounting for the non-linear terms (Moramarco et al., 2008ab; Aricò and Nasello, 2018; Zheng et al., 2020). Conversely, the applicability conditions of the approximated models for mud-flows were not so deeply analysed. Starting from the theoretical results of Di Cristo et al. (2013a),

applicability criteria for some approximate models were deduced in Di Cristo et al. (2014a), Di Cristo et al. (2014b) for both a Herschel & Bulkley and a power-law rheology through an analysis of the linearized equations. Moreover, in Di Cristo et al. (2018a), accounting for the non-linear terms, the applicability conditions of both Kinematic and Diffusive approximate models have been defined for a power-law fluid studying the analytical solution of the steady problem. Applicability criteria have been derived in terms of two non-dimensional parameters governing the problem: the Froude and Kinematic wave numbers. It has been also shown that the criteria deduced for clear-water flows (Moramarco et al., 2008a) cannot be straightforwardly applied to mud-flows for both Diffusive and Kinematic approximate models because they lead to non-conservative predictions, in particular for small power-law index values (Di Cristo et al., 2018a). A further analysis performed by Di Cristo et al. (2019), comparing the unsteady numerical results of the fully non-linear model with the corresponding ones deduced through the KWM, has confirmed these conclusions. In this unsteady analysis, the criteria for the application of the KWM have been provided in terms of the hydrograph rising time. The present paper extends the non-linear unsteady analysis of Di Cristo et al. (2019) to the DWM, considering discharge hydrographs at the channel inlet characterized by different wave durations. The objective is to provide applicability criteria of the DWM for a shear-thinning power-law fluid described by the model proposed by Ng and Mei (1994). In the study, carried out through an unsteady numerical analysis of both the Full and the Diffusive Wave Models, the performance of the DWM are evaluated considering the dimensionless error on the maximum flow depth and on the maximum discharge.

The paper is organized as follows. Section 2 reports the governing equations for the FWM and of the DWM and the adopted numerical methods. Section 3 illustrates the performed tests and the results of the comparison between the FWM and the DWM, along with the obtained applicability criteria. An exemplification of the proposed methodology is illustrated in Section 4. Finally, conclusions are drawn in Section 5.

2. Unsteady analysis

2.1. Full wave Model

A homogeneous layer of an incompressible shear-thinning power-law fluid flowing over a fixed bed, with a constant inclination (θ) with respect to the horizontal plane, without lateral inflow or outflow is investigated. Neglecting the surface tension and considering a laminar gradually varied flow where spatial variations occur over scales larger than flow depth, so that flow resistance by the sidewalls is negligible with respect to that by the bottom, the dimensional depth-averaged mass and momentum conservation equations are (Ng and Mei, 1994; Di Cristo et al., 2017):

$$\frac{\partial \widetilde{h}}{\partial \widetilde{t}} + \frac{\partial \widetilde{q}}{\partial \widetilde{x}} = 0 \tag{1}$$

$$\frac{\partial \widetilde{q}}{\partial \widetilde{t}} + \beta \frac{\partial}{\partial \widetilde{x}} \left(\frac{\widetilde{q}^2}{\widetilde{h}} \right) + g\widetilde{h} \frac{\partial \widetilde{h}}{\partial \widetilde{x}} cos\theta = g\widetilde{h} sin\theta - \frac{\widetilde{\tau}_b}{\rho} \tag{2}$$

where $\widetilde{t}$ is the time, $\widetilde{x}$ is the streamwise coordinate, $\widetilde{h}$ the flow depth, $\widetilde{q}$ the flow rate (for unit of width), g and ρ the gravity and the fluid density, respectively. β and $\widetilde{\tau}_b$ are the momentum correction factor and the bottom stress, respectively. In laminar regime the expressions of the momentum correction factor and of the bottom stress are (Ng and Mei 1994; Di Cristo et al., 2013b), respectively:

$$\beta = 2\frac{2n+1}{3n+2} > 1 \tag{3}$$

$$\widetilde{\tau}_b = \mu_n \left(\frac{2n+1}{n} \frac{\widetilde{u}}{\widetilde{h}} \right)^n \tag{4}$$

being $\widetilde{u} = \widetilde{q}/\widetilde{h}$ the depth-averaged velocity; μ_n and n the consistency and the rheological index of the power-law fluid, respectively. For shear-thinning fluids the rheological index is smaller than one, while values larger than one represent shear-thickening fluids. In the following, only shear-thinning fluids have been considered.

The following dimensionless variables are introduced:

$$x = \widetilde{x}/\widetilde{L} \quad h = \widetilde{h}/\widetilde{h}_N \quad q = \widetilde{q}/\widetilde{q}_{ref} \quad t = \widetilde{T}/\widetilde{T}_{ref} \tag{5}$$

where $\widetilde{L}$ is the dimensional channel length, $\widetilde{q}_{ref}$ is the reference flow rate for unit width and $\widetilde{h}_N$ the corresponding dimensional normal, i.e. uniform, depth. The reference time scale $\widetilde{T}_{ref}$ is assumed equal to the kinematic wave channel travel-time of the reference discharge (Moramarco et al., 2008b):

$$\widetilde{T}_{ref} = \frac{\widetilde{L}}{\widetilde{C}_{KWM}} \tag{6}$$

where $\widetilde{C}_{KWM}$ denotes the dimensional celerity of the kinematic wave, which for power-law fluid reads (Di Cristo et al., 2018b):

$$\widetilde{C}_{KWM} = C_{KWM} \frac{\widetilde{q}_{ref}}{\widetilde{h}_N} \quad \text{with} \quad C_{KWM} = \frac{2n+1}{n} \tag{7}$$

C_{KWM} being the dimensionless celerity.

Accounting for (5)–(7), Eqs. (1)–(2) may be rewritten in dimensionless form as:

$$C_{KWM} \frac{\partial h}{\partial t} + \frac{\partial q}{\partial x} = 0 \tag{8}$$

$$C_{KWM} \frac{\partial q}{\partial t} + \beta \frac{\partial}{\partial x} \left(\frac{q^2}{h} \right) = -\frac{1}{F^2} \frac{\partial}{\partial x} \left(\frac{h^2}{2} \right) + Kh \left(1 - \frac{q^n}{h^{2n+1}} \right) \tag{9}$$

In Eq. (9) F denotes the normal Froude number and K the kinematic wave number, whose expressions are:

$$F = \frac{\widetilde{q}_{ref}}{\widetilde{h}_N^{3/2} \sqrt{g\cos\theta}} \tag{10}$$

$$K = \frac{1}{F^2} \frac{\widetilde{L}}{\widetilde{h}_N} \tan\theta \tag{11}$$

Therefore, as in the clear-water case (Govindaraju et al., 1988a, 1988b; Moramarco et al., 2008a), for the power-law fluids the problem is univocally defined through the two dimensionless numbers (F, K) or equivalently (F, KF^2).

As reported with more details in Di Cristo et al. (2019), the system (8)–(9) has been numerically solved using an explicit first-order Euler scheme for the temporal discretization and a second-order Finite-Volume method for the spatial discretization.

2.2. Diffusive Wave Model

The DWM is obtained neglecting in Eq. (9) the local and convective inertia terms, represented by the first two terms at the l.h.s., obtaining:

$$\frac{\partial h}{\partial x} = KF^2 \left(1 - \frac{q^n}{h^{2n+1}} \right) \tag{12}$$

Taking the spatial (resp. temporal) derivative of Eqs. (8) (resp. of Eq. (12)), the DWM may be rewritten into the advection–diffusion form as follows:

$$\frac{\partial q}{\partial t} + c \frac{\partial q}{\partial x} = v \frac{\partial^2 q}{\partial x^2} \tag{13}$$

.where the expressions of the advective velocity (c) and of the hydraulic diffusivity (v) are:

$$c = \frac{2n+1}{n} \frac{q}{h} \quad v = \frac{1}{nKF^2} \frac{h^{2n+1}}{q^{n-1}} \tag{14}$$

The influence of the power-law index value on both the advective velocity and the hydraulic diffusivity has been discussed through a linear analysis by Di Cristo et al. (2018b) and in the non-linear conditions by Pascal (1991), in studying the stability of power-law fluid gravity flows of over a plane.

The DWM, i.e. Eqs. (8) and (12), has been numerically solved in implicit way through a Finite-Volume scheme. The scheme is first-order both in space and in time. A Newton-Raphson iterative procedure has been used to solve the non-linear algebraic system.

2.3. Boundary conditions

For both models, a flow hydrograph is imposed as the upstream boundary condition, whose duration $\widetilde{T}_f$ is expressed as a multiple of the reference time scale, i.e. $\widetilde{T}_f = m\widetilde{T}_{ref}$, so that the value of m, assumed larger than one, represents the dimensionless duration of the upstream hydrograph.

The hydrograph shape has been assigned accordingly to the following four-parameters Pearson type III distribution (Moramarco et al., 2008a; Di Cristo et al., 2019):

$$q(0,t) = q_p t^{\frac{1}{\gamma-1}} e^{\left(\frac{1-t}{\gamma-1} \right)} \tag{15}$$

where q_p is the dimensionless peak discharge for unit width and γ is the dimensionless shape factor, with two different values for the rising ($\gamma = \gamma_{ris}$ for $t < 1$) and the recession ($\gamma = \gamma_{rec}$ for $t > 1$) limbs, respectively. q_p is assumed equal to 2 and γ_{ris} equal to 1.3. The γ_{rec} value is defined imposing that the value of the discharge, averaged in time over the duration m, equals the dimensionless reference discharge ($\widetilde{q}_{ref} = 1$). Zucco et al. (2015) showed that the adopted hydrograph well represents the single-peak floods occurring in natural channels. Moreover, it may be considered also representative for debris/mud flows, based on the correlation between debris/mud flow and water flow discharge (Takahashi, 1991; VanDine, 1985; Chen et al., 2008).

As far as FWM is concerned, whenever hypercritical conditions occur at the channel inlet, an additional boundary condition is required and, imposing the instantaneous validity of the normal flow rating curve, the following flow depth value is assigned:

$$h_0 = q(0, t)^{\frac{n}{2n+1}} \tag{16}$$

At the channel outlet, for both models the critical flow depth is imposed which, for a power-law fluid, reads (Di Cristo et al., 2019):

$$h_c = \sqrt[3]{\beta q^2 F^2} \tag{17}$$

3. Numerical tests

3.1. Criteria for the DWM applicability

The prediction of the maximum values of the hydraulic variables such as flow depth and rate constitutes the essence of a typical hazard assessment. From this standpoint, the capacity of the DWM in reproducing the results of the FWM is tested in terms of mean values along the channel of relative errors on the maximum flow depth and maximum discharge (ε_h and ε_q) denoted with ε_h^* and ε_q^*, respectively. ε_h and ε_q

are evaluated along the x axis as (Moramarco et al., 2008b):

$$\varepsilon_h(x) = \frac{h_{max}^{DWM}(x) - h_{max}^{FWM}(x)}{h_{max}^{FWM}(x)} 100 \qquad \varepsilon_q(x) = \frac{q_{max}^{DWM}(x) - q_{max}^{FWM}(x)}{q_{max}^{FWM}(x)} 100 \qquad (18)$$

where h_{max}^{FWM} and h_{max}^{DWM} (resp. q_{max}^{FWM} and q_{max}^{DWM}) are the dimensionless maximum flow depth (resp. flow rate) computed by the FWM and the DWM, respectively. With the aim of excluding the regions where the boundary conditions may have a large influence, ε_h^* and ε_q^* are computed limitedly to $0.05 \leq x \leq 0.95$ (Moramarco et al., 2008b). A positive mean error indicates that, on average along the channel, the DWM overestimates the flow depth (or discharge) predicted by the FWM, while negative value results in an averaged underestimation, which for a typical flow routing problem represents a non-conservative prediction.

3.2. Performed tests

Several numerical tests have been performed under a variety of flow conditions, characterized by different synthetic inlet hydrographs. Different tests have been carried out varying the hydrograph duration from 5 to 20000. Correspondingly, the γ_{rec} value ranges between 1.1 ($m = 5$) and 12,536 ($m = 20000$). The rheological index has been varied in the whole shear-thinning range, namely $n \leq 1$, the normal Froude number covers the hypocritical range. Finally, in the tests the kinematic wave number has been varied from 5 up to 100. All simulations have been performed with the same spatial step $\Delta x = 0.005$, while the time step was equal to $\Delta t = 10 \cdot 10^{-7}$ for the FWM and $\Delta t = 10 \cdot 10^{-4}$ for the DWM. The accuracy of the numerical solutions has been tested verifying the independence of the simulation results when reducing the spatial and temporal step values. In particular, halving both the mesh spacing and the time step, the differences on ε_h^* and ε_q^* are below 0.1% and 0.2%, respectively.

4. Results and discussion

Figs. 1 and 2 report the mean error of the maximum flow depth and discharge, ε_h^* and ε_q^*, respectively, as a function of the hydrograph duration, m, for $F = 0.25$ and for four different rheological indexes values, i.e. $n = 0.25, 0.50, 0.75, 1.00$. Two different values of the kinematic number have been considered, namely $K = 5$ (a) and $K = 16$ (b).

Independently of the kinematic wave number and the power-law index value, Fig. 1 shows that ε_h^* monotonically decreases with m, asymptotically reaching its minimum negative value. Such a value

corresponds to the quasi-steady conditions, $\varepsilon_{h,qs}^*$, reported as red horizontal lines in Fig. 1, and it coincides with the averaged flow depth error evaluated assuming valid in each instant the steady solution (Di Cristo et al., 2019). Such a monotone behavior has been verified for all the investigated (F, K, n) triplets (results not shown for the sake of brevity).

The DWM differs from FWM for the inertial terms in the moment equation, i.e. l.h.s. of Eq. (9). Since for high values of m the local inertia becomes negligible, Fig. 1 shows that ignoring the convective inertial term an underestimation of flow depth has induced and then negative values of ε_h^* are observed. For shorter hydrograph durations, the local inertia progressively attenuates this underestimation. Indeed, small values of m, i.e. short hydrograph durations, are characterized by an overestimation of flow depth and positive values of ε_h^*.

In this study the DWM is assumed to be conservatively applied for positive mean error values, representing a flow depth overestimation. Conversely, negative values of ε_h^*, corresponding to an underestimation on the maximum flow depth, imply a non-conservative application of the DWM. In what follows, the DWM is considered safely applicable provided that the negative values of ε_h^* are larger than a prescribed threshold value. As in previous studies (Moramarco et al., 2008b; Di Cristo et al., 2019), this threshold is assumed equal to 5% and therefore the DWM would be considered applicable whenever $\varepsilon_h^* > -5\%$. Considering the monotone dependence of ε_h^* on m and that the minimum value of ε_h^* corresponds to the asymptotic value $\varepsilon_{h,min}^* = \varepsilon_{h,qs}^*$, the condition $\varepsilon_{h,qs}^* > -5\%$ guarantees the applicability of the DWM independently of the hydrograph duration. For instance, Fig. 1 shows that, for $F = 0.25$ and $K = 5$ and $K = 16$, the DWM may be safely applied for all the m values only for the case corresponding to a Newtonian fluid, i.e. $n = 1$, and K equal to 16 (see Fig. 1b). In all the other cases reported in Fig. 1, since $\varepsilon_{h,qs}^* < -5\%$, the condition $\varepsilon_h^* \geq -5\%$ defines an upper bound of m for the applicability of the DWM in terms of error on the maximum depth, $m_{h,max}$.

As far as the mean error on the maximum discharge ε_q^* is concerned, Fig. 2 shows that, independently of the K and n values, ε_q^* has a non-monotone behavior with the hydrograph duration. Starting from a value $\left(\varepsilon_{q,min}^*\right)$ pertaining to the lowest investigated m value, ε_q^* monotonically increases up to a maximum (always positive) value and subsequently decreases vanishing for sufficiently large hydrograph durations. The zero asymptotic value is again consistent with the quasi-steady approximation $\left(\varepsilon_{q,qs}^* = 0\right)$. The above described functional dependence of ε_q^* on m has been found for all the investigated Froude
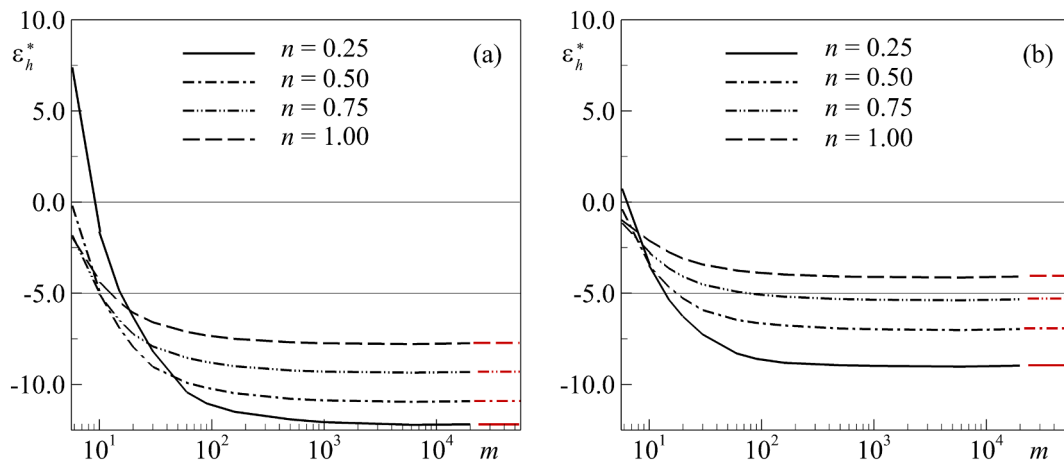

Fig. 1. Flow depth mean error as a function of the wave duration for four different rheological indexes, $n = 0.25, 0.5, 0.75, 1.0$ ($F = 0.25$). a) $K = 5$; b) $K = 16$. Red horizontal lines correspond to the quasi-steady condition $\varepsilon_{h,qs}^*$(For interpretation of the references to colour in this figure legend, the reader is referred to the web version of this article.).
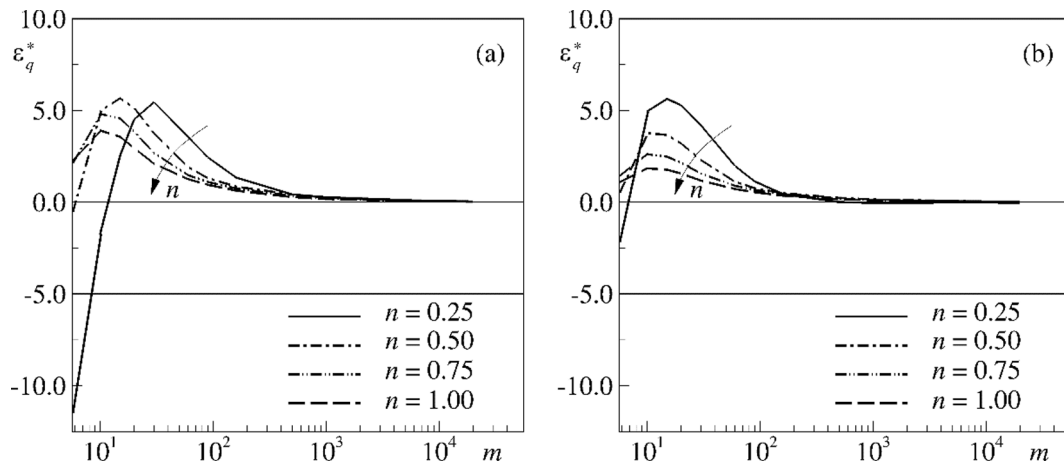
Fig. 2. Discharge mean error as a function of the wave duration for four different rheological indexes, $n = 0.25, 0.5, 0.75, 1.0$ ($F = 0.25$). a) $K = 5$; b) $K = 16$.

and kinematic wave numbers values, and independently of the value of the power-law exponent (results not shown).

If $\varepsilon^*_{q,min}$ is larger than -5%, the DWM may be safely applied for all wave durations. For instance, for $K = 16$ (Fig. 2b) such a condition holds for all the considered n values, while for $K = 5$ (Fig. 2a) only whenever n is larger than 0.25. In particular, a further investigation has shown that $\varepsilon^*_{q,min}$ is still smaller than -5% for $n = 0.45$. When $\varepsilon^*_{q,min} < -5\%$ (see for instance the $K = 5$ and $n = 0.25$ case in Fig. 2a), there exists a lower bound of m for the safe application of the DWM in predicting the discharge, $m_{q,min}$.

Inspecting Fig. 1a and 1b, it is also noted that for a fixed value of the (F, n) pair and of the hydrograph duration m, as K increases $\varepsilon^*_{h,min}$ (negative value) increases. In general, numerical analyses have confirmed that the absolute value of errors in terms of both flow depth and discharge decreases for increasing K. This can be explained considering that an increase of K induces in both full (Eq. (9)) and diffusive (Eq. (12)) momentum equations an increase of the source term (difference between effects of gravity and friction).

In conclusion, when $\varepsilon^*_{h,min} > -5\%$ (resp. $\varepsilon^*_{q,min} > -5\%$) the DWM can be safely applied to predict the flow depth (resp. discharge) for all hydrograph durations. Conversely, when $\varepsilon^*_{h,min} < -5\%$ (resp. $\varepsilon^*_{q,min} < -5\%$) there exists an upper bound, $m_{h,max}$ (resp. a lower bound, $m_{q,min}$) for the hydrograph duration in order to safely apply the DWM for predicting the flow depth (resp. the discharge). In this case, an analysis aimed to individuate the values of triplet (K, n, F) for which $\varepsilon^*_{h,min}$ and $\varepsilon^*_{q,min}$ are larger than -5% has been carried out.

In particular, for given values of F and n, analyzing the results in quasi-steady conditions, the value of K for which $\varepsilon^*_{h,min}$ equals -5% has been determined. Denoting with $\overline{K}_h$ this value, it follows that the DWM is applicable for hydrograph of any duration in terms of maximum flow depth whenever $K \geq \overline{K}_h$. Similarly, the analysis of the results at $m = 5$ has led to define the value of K for which $\varepsilon^*_{q,min}$ is equal to -5%, denoted with $\overline{K}_q$. Fig. 3 reports for several values of n, i.e. $n = 0.25, 0.5, 0.75, 1.0$, and for Froude number $F \geq 0.1$, the values of the limiting kinematic wave numbers $\overline{K}_h$ and $\overline{K}_q$. In this map the applicability region is represented by the area on the right of $\overline{K}_h$ and $\overline{K}_q$ lines. For all hydrograph durations, the DWM can be safely applied to predict both flow depth and discharge whenever K is larger than both $\overline{K}_h$ and $\overline{K}_q$, i.e. $\overline{K} = \max\left\{\overline{K}_h, \overline{K}_q\right\}$.

Fig. 3 shows that for all n values there exists a $\overline{K}_h$ value, and it decreases as the Froude number increases. This observation implies that the applicability range of the DWM in terms of maximum flow depth
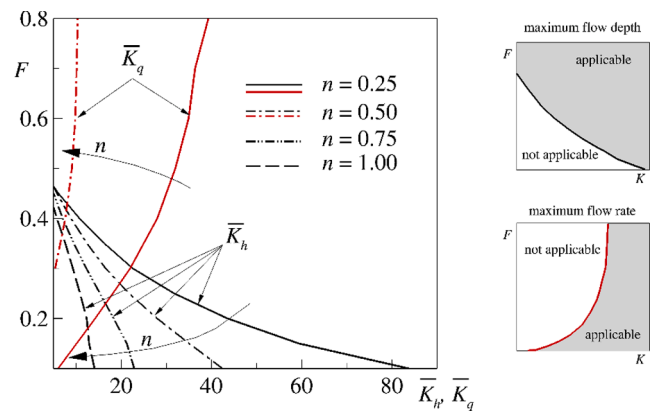

Fig. 3. Limiting values of the kinematic wave number numbers $\overline{K}_h$ and $\overline{K}_q$ Vs the Froude number. Black lines: $\overline{K}_h$; Red lines: $\overline{K}_q$. (For interpretation of the references to colour in this figure legend, the reader is referred to the web version of this article.)

enlarges with the Froude number. For Froude number larger than 0.45 the applicability of the DWM holds for all considered rheologies. For fixed value of Froude number, an increase of the power-law index leads to a strong enlargement of the applicability region, i.e. $\overline{K}_h$ reduces with n. For instance, for $F = 0.1$, increasing n from 0.25 up to 1.0 leads to a reduction of $\overline{K}_h$ from 84 to 14.

About the discharge, in the investigated range of the governing parameters, for $n > 0.5$ the DWM is always applicable independently of the wave duration. Only for $n \leq 0.5$ a lower bound of the kinematic wave number for the discharge prediction $\overline{K}_q$ exists as shown in Fig. 2. Furthermore, differently from the flow depth, $\overline{K}_q$ increases with F, and therefore the applicability region of the DWM for the discharge shrinks with the Froude number. For a fixed Froude number, the dependence of $\overline{K}_q$ on the power-law index is similar to the one of $\overline{K}_h$, i.e. a reduction of n increases the $\overline{K}_q$ value. For instance, for $F = 0.8$, increasing n from 0.25 up to 0.5, $\overline{K}_q$ reduces from 40 to 10. As far as the prediction of both flow depth and discharge is concerned, Fig. 3 indicates that for $n > 0.5$ the lower bound of the kinematic wave number $\overline{K}$ coincides with $\overline{K}_h$, therefore for Froude number larger than 0.45 and $n > 0.5$ the DWM is applicable both in terms of flow depth and discharge for all m values. A different conclusion holds for $n \leq 0.5$. Indeed, at large F numbers, the applicability range is bounded by $\overline{K}_q$, conversely for low Froude number value the limiting values $\overline{K}_h$ is more restrictive. As consequence for small values of n a non-monotone dependence of $\overline{K}$ on the Froude number is

found. For instance, at $n = 0.25$ the minimum value of $\overline{K}$ is detected at $F = 0.3$ ($\overline{K} \cong 23$).

With the aim of defining the DWM applicability conditions for K smaller than $\overline{K}_h$ or $\overline{K}_q$, the influence of the hydrograph duration has been investigated. As previously discussed, an upper (lower) bound $m_{h,max}$ ($m_{q,min}$) of the hydrograph duration has to be respected for the safe application of DWM in predicting the flow depth (discharge). Those bounds depend on the values of the Froude and kinematic wave numbers along with the power-law exponent and they been computed starting from the results of the numerical simulations.

As far as the flow depth is concerned, for each power-law index value considered in Fig. 3, accounting for the results in terms of $\overline{K}_h$, Froude numbers up to 0.4 have been investigated. For each (F, n) pair, the DWM may be applied for maximum flow depth prediction whenever $m \leqslant m_{h,max}$. Fig. 4 reports the $m_{h,max}$ values as function of the kinematic wave number K for the considered rheological indexes, $n = 0.25, 0.5, 0.75, 1.0$ and for (a) $F = 0.1$, (b) $F = 0.2$, (c) $F = 0.3$, (d) $F = 0.4$. The (K, m) pairs on the right of each curve corresponds to applicability conditions. Consistently with the conclusion that for $K \geqslant \overline{K}_h$, the DWM can be safely applied for all wave durations, the curves in Fig. 4 diverge as K approaches $\overline{K}_h$. As far as the discharge is concerned, owing to the results in terms of $\overline{K}_q$ of Fig. 3, for identifying the $m_{q,min}$ values, the investigated Froude number range has been extended up to 0.8, while only the power-law index 0.25 and 0.5 have been considered. Fig. 5 reports the $m_{q,min}$ values as a function of the kinematic wave number K for Froude numbers ranging between 0.1 and 0.8 and rheological indexes $n = 0.25$ (a) and 0.5 (b). For each (F, n) pair, the DWM may be applied for maximum discharge prediction whenever $m \geqslant m_{q,min}$ and therefore the

region above each curve individuates the applicability domain.

The comparison between Figs. 4 and 5 reveals that $m_{h,max}$ extends over one or two orders of magnitude whereas $m_{q,min}$ spans about ten. Moreover, for a fixed value of the Froude number, the applicability region both in terms of flow depth and flow rate enlarges for increasing K and n. The dependence on the Froude number is different. For a fixed value of n, the applicability region for the maximum flow depth (resp. flow rate) prediction enlarges (resp. shrinks) when the Froude number is increased. Both conclusions agree with the results shown in Fig. 3.

The effects of the power-law exponent and the kinematic wave number on the applicability regions may be easily explained analyzing the magnitude of the terms of Eq. (9), since the DWM is expected to approximate better the FWM, whenever the inertial terms at the left-hand side of Eq. (9) are smaller than the ones at right-hand side.

The rheological index n influences the two l.h.s. terms and the source term at r.h.s. With regards to the inertial terms, Fig. 6 depicts C_{KWM} and β as functions of the power-law index. Fig. 6 suggests that n marginally affects the coefficient of the convective inertia term, β, while the reduction the power-law exponent strongly increases the weight of the local inertia through C_{KWM}. This behavior contributes to the reduction of the DWM applicability area as n decreases (Figs. 4 and 5).

Moreover, the influence of the power-law exponent on the source term $S(q, h) = Kh \left(1 - \frac{q^n}{h^{2n+1}}\right)$ is illustrated in Fig. 7, by plotting the *iso-contours* of $S(q, h)$ for two values of the power-law index, namely $n = 0.25$ and $n = 1.0$, and assuming a conservative unitary value of the kinematic wave number. The comparison between Fig. 7a and 7b suggests that the magnitude of the source term is substantially larger for $n = 1.0$
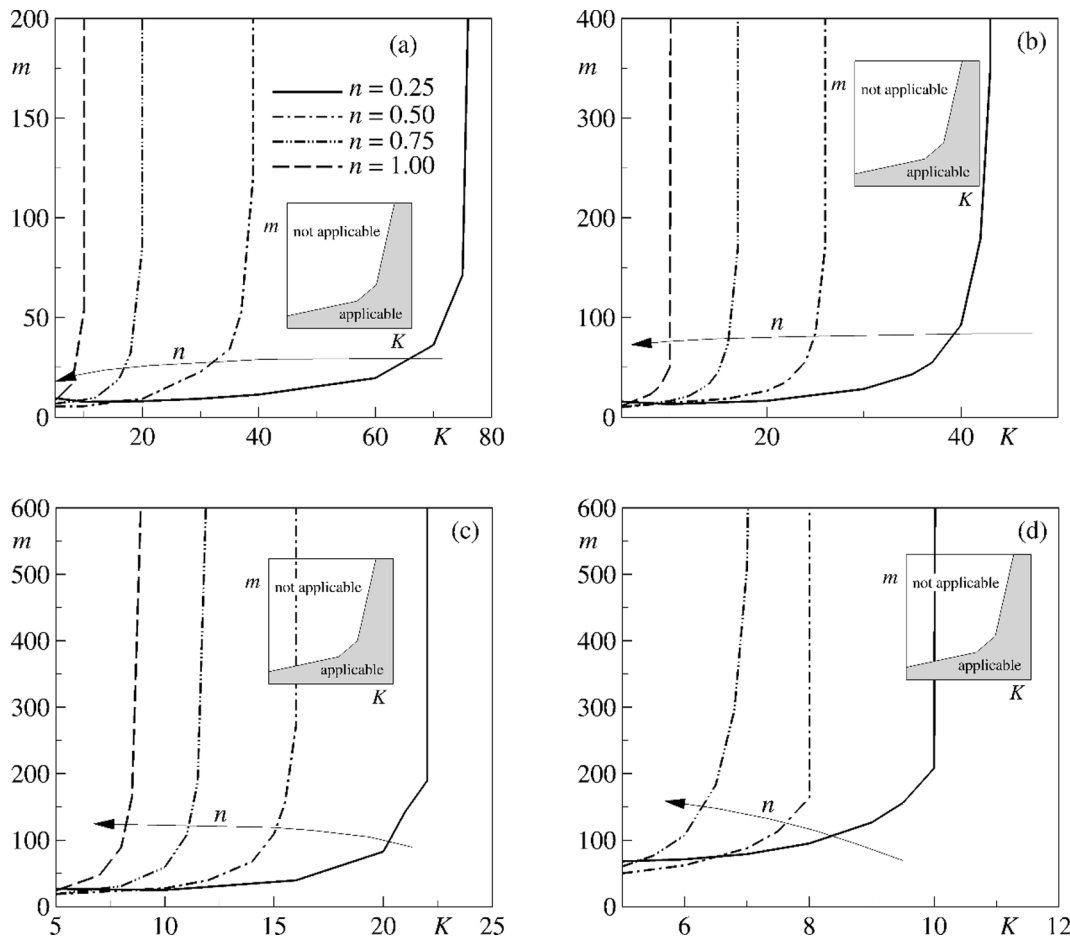

Fig. 4. Upper bound $m_{h,max}$ for DWM applicability in terms of maximum flow depth as function of the kinematic wave number K for different rheological indexes, $n = 0.25, 0.5, 0.75, 1.0$ and for (a) $F = 0.1$, (b) $F = 0.2$, (c) $F = 0.3$, (d) $F = 0.4$.
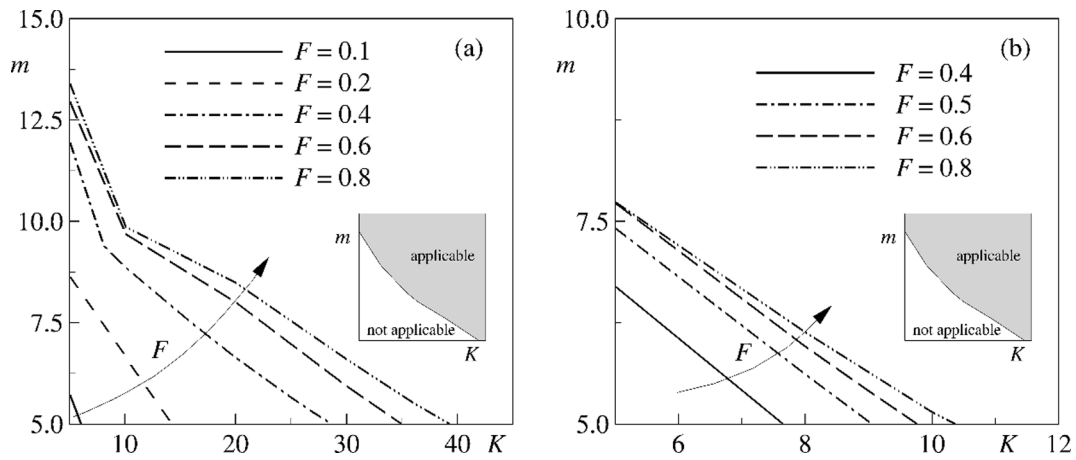
Fig. 5. Lower bound $m_{q,min}$ for DWM applicability in terms of maximum discharge as function of the kinematic wave number K for F ranging between 0.1 and 0.8 and two rheological indexes: (a) $n = 0.25$, (b) $n = 0.50$.
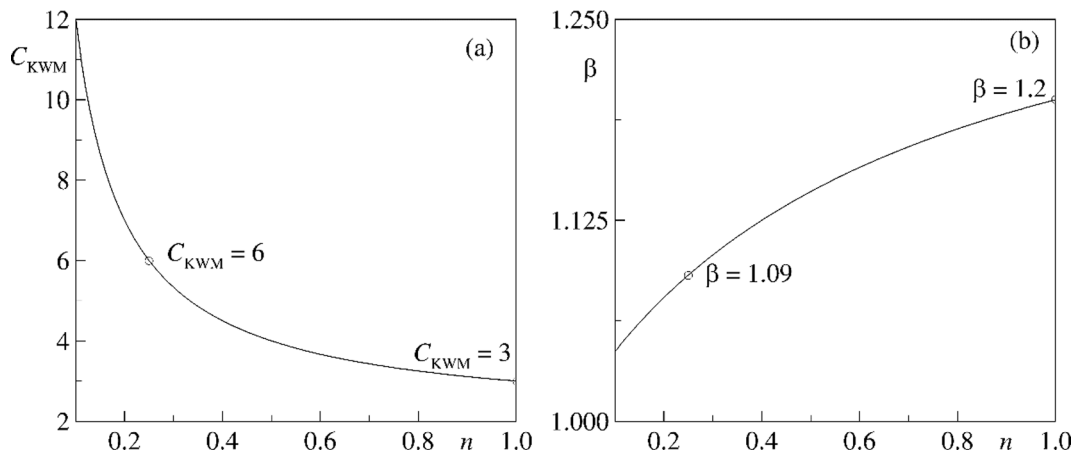

Fig. 6. Dimensionless celerity C_{KWM}, (a), and coefficient of the convective inertia, β, (b) as function of the rheological index.
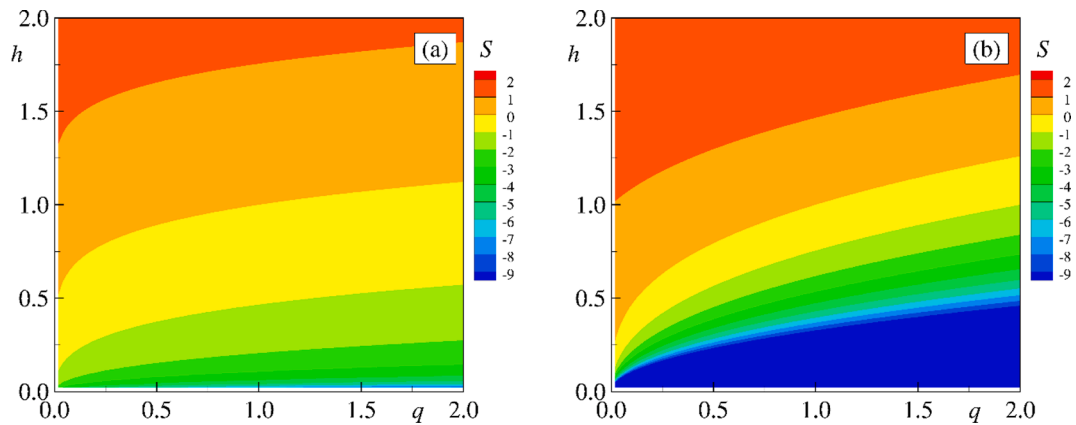

Fig. 7. Source term values as function of the discharge and flow depth for two rheological indexes: (a) $n = 0.25$, (b) $n = 1.00$.

than for $n = 0.25$, particularly for small values of the flow depth. This behavior contributes to reduce the DWM applicability domain as n decreases.

Finally, for a fixed value of n and independently of the value of the (q, h) pair, S linearly increases with K, which justifies the corresponding enlargement of the DWM applicability region.

Conversely, the effect of the Froude number on the applicability bounds $m_{h,max}$ and $m_{q,min}$ is more complex. In fact, the Froude number

influences both the weight of the r.h.s. of Eq. (9) and the boundary condition at the channel outlet (Eq. (17)). Indeed, a reduction of F causes the weight of the pressure differential term to increase, and similarly the magnitude of the r.h.s. of Eq. (9). At the same time, it also leads to a reduction of the critical flow depth at the channel outlet, with a not easily foreseeable effect on the relative error in terms of both maximum flow depth and flow rate.

The above results allow to define the DWM applicability conditions

analyzing the mean error along the channel length. Indeed, although present results are useful for hazard assessment at large scales, such as the basin one, the criteria fulfillment does not ensure that the DWM may accurately describe the spatio/temporal dynamics of the hydrograph. A systematic comparison of FWM and DWM under this perspective is out of the scope of the present research. However, in order to give an idea about the local and instantaneous error in the DWM application, a flow condition, in which the criterion is fulfilled, has been analysed in detail. The following condition has been considered: $n = 0.25$, $F = 0.2$, $K = 20$, $m = 16$, for which $\varepsilon_h^* = -5\%$ and $\varepsilon_q^* = 5\%$. Fig. 8 compares the time evolutions of the flow depth (Fig. 8a) and discharge (Fig. 8b) predicted by the two methods at three channel locations, namely $x = 0.25$, $x = 0.5$ and $x = 0.75$.

Fig. 8a shows that while the DWM correctly predicts the celerity of the front, some differences are visible in terms of celerity of the maximum value of flow depth. Indeed, the flow depth peak moves slightly faster in the DWM than in the FWM. From Fig. 8b, some differences are still observed in terms of celerity of maximum discharge, but the trend is less clear with the peaks of the DWM that move slightly faster in the first half of the channel and slower downstream. Fig. 8 also clearly indicates that for the considered condition, negative value of ε_h^* and positive values of ε_q^* correspond to a DWM underprediction of maximum of flow depth and overprediction of the maximum discharge, respectively. To quantify the performance of the DWM in reproducing the spatio/temporal dynamics of the hydrograph, several indices have been considered. Firstly, the Nash–Sutcliffe efficiency index (Nash and Sutcliffe 1970):

$$NS_q = \left[1 - \frac{\sum_t (q^{FWM}(t) - q^{DWM}(t))^2}{\sum_t (q^{FWM}(t) - \overline{q}^{FWM})^2}\right] \cdot 100 \qquad (19)$$

has been analyzed. In Eq. (19) $q^{FWM}(t)$ and $q^{DWM}(t)$ are the dimensionless instantaneous flow rates computed by the FWM and the DWM, respectively, in a given section and $\overline{q}^{FWM}$ is the FWM discharge mean value in the same section. In addition, the the local values of ε_h and ε_q have been computed along with the relative errors on the time to peak flow depth (t_{h_p}) and discharge (t_{q_p}), expressed as

$$\varepsilon_{t_{h_p}} = \left(\frac{t_{h_p}^{DWM} - t_{h_p}^{FWM}}{t_{h_p}^{FWM}}\right) \cdot 100 \qquad \varepsilon_{t_{q_p}} = \left(\frac{t_{q_p}^{DWM} - t_{q_p}^{FWM}}{t_{q_p}^{FWM}}\right) \cdot 100 \qquad (20)$$

Table 1 reports the values of the considered five indices at the three sections represented in Fig. 8.

The very high values of the NS_q index indicate very good reproduction of the hydrograph shape by the DWM. The relative errors on the estimation of the maximum flow depth and discharge show that the differences between the peak values, i.e. the underprediction of the

Table 1

NS_q index, relative errors ε_h and ε_q, $\varepsilon_{t_{h_p}}$ and $\varepsilon_{t_{q_p}}$ at three different abscissas $x = 0.25$, $x = 0.5$, $x = 0.75$ for the condition $n = 0.25$, $F = 0.2$, $K = 20$, $m = 16$.

	$x = 0.25$	$x = 0.5$	$x = 0.75$
NS_q	99.9%	99.4%	99.1%
ε_h	−2.3%	−4.4%	−7.4%
ε_q	0.8%	5.7%	9.2%
$\varepsilon_{t_{h_p}}$	−18.6%	−9.0%	−11.5%
$\varepsilon_{t_{q_p}}$	10.8%	11.9%	−13.8%

maximum flow depth and the overprediction of discharge, are within 10% and increase along the channel. For the time to peak of flow depth and discharge, the relative errors are between 10% and 20%. Present results suggest that criteria deduced analyzing the spatially averaged errors, such as the one herein presented, have to be applied with caution whenever a detailed information about the hydrograph dynamics is required. In other words, there is not a univocal way to assess the applicability of the DWM, but different criteria can be defined by selecting appropriate error parameters for the considered application.

4.1. An example of application: The Cervinara mud-flows

In order to show that the DWM applicability conditions can be satisfied in real mud-flows, the historical event occurred in 1999 in Cervinara (Southern Italy) is considered. The area was hit by prolonged heavy rains and their action over the pyroclastic deposits covering the hills triggered several mud-flows which reached the town center causing damages and fatalities. Two episodes form this dramatic series are considered in the following to provide an example of the possible application of the above methodology, namely the two mud-flows arising from the Iozzino and San Gennaro watersheds (Cascini et al., 2011).

Based on the experiments by Carotenuto et al. (2015), the power-law model can be adopted to describe the rheology of the muds developed after the intense washing of pyroclastic deposits. From the rheological study the value of the consistency and of the rheological exponent have resulted equal to $\mu_n = 21.4$ Pa s^n and to $n = 0.1$, respectively. Based on the hydrological data and on the results of the simulations reported by Cascini et al. (2011), the peak unit width discharges have been estimated as $q_{ref} = 0.011 \text{m}^2/\text{s}$ for Ioffredo watershed and $q_{ref} = 0.033 \text{m}^2/\text{s}$ for San Gennaro one. The typical values of the longitudinal slope and flow width in the urbanized area have been estimated from available cartography as $\theta = 0.049$ for and $\theta = 0.032$ for the Ioffredo and San Gennaro watersheds, respectively. Combining the above data with the bottom shear stress relationship (Eq. (4)), the reference Froude
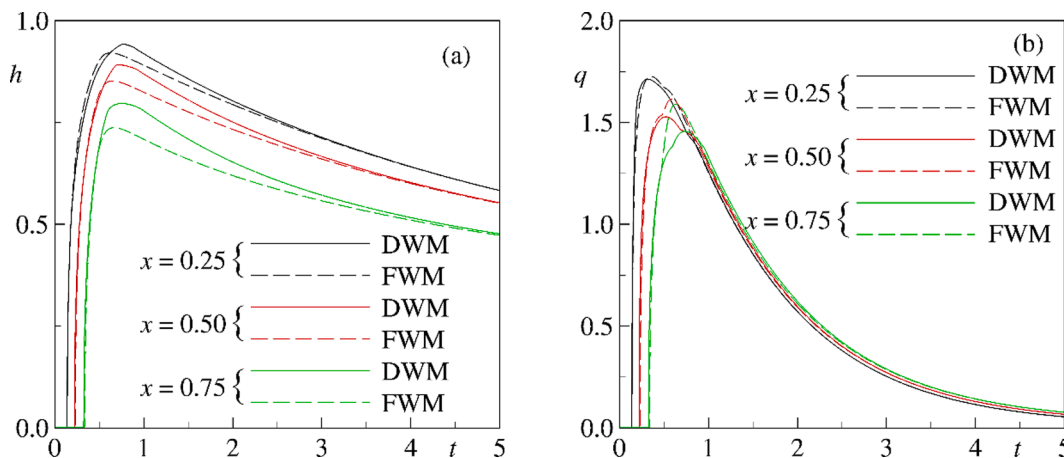

Fig. 8. Time evolution of flow depth (a) and discharge (b) at three different abscissas $x = 0.25$, $x = 0.5$, $x = 0.75$ for the condition $n = 0.25$, $F = 0.2$, $K = 20$, $m = 16$.

Table 2
Flow characteristics of the considered example.

Watershed	μ_n	n	θ	$\widetilde{h}_N$	$\widetilde{q}_{ref}$	F
	(Pa s^n)	(-)	(rad)	(m)	(m^2/s)	(-)
Ioffredo	21.4	0.1	0.049	0.040	0.011	0.45
San Gennaro			0.032	0.065	0.033	0.65

number has been evaluated from Eq. (8) as $F = 0.45$ and $F = 0.65$ for the two mudflows. The main data characterizing the two examples are summarized in Table 2.

The evaluation of the $\overline{K}_h$ value for the considered rheology confirmed the effect of the shear-thinning behavior. As indicated in Fig. 3, for both values of the Froude number it results $\overline{K}_h \leqslant 5$, implying that the criterion on the mean values of the dimensionless error on the maximum flow depth is satisfied for any meaningful value of the channel length and for any duration of the flow hydrograph. As far as the criterion on the mean values of the dimensionless error on the maximum flow discharge is concerned, the values of $\overline{K}_q$ have been computed as 44.8 and 43.4, for the events resulting from Ioffredo and San Gennaro watersheds, respectively. With these threshold values the DWM is applicable, independently of the hydrograph duration, in reaches with lengths longer than 50 m.

5. Conclusions

The present study investigates the applicability of the Diffusive Wave Model (DWM) in predicting the unsteady propagation of a mud-flow wave, represented through a shear-thinning power-law fluid, described through the model proposed by Ng and Mei (1994). The analysis accounts for the non-linearity of the governing equations, which have been numerically solved. For the Full Wave Model (FWM) an explicit first-order scheme in time and a second-order Finite-Volume method for the spatial discretization has been adopted. The DWM has been numerically solved with an implicit Finite-Volume scheme with a first-order in space and time approximation.

Different tests have been performed varying the wave duration of the hydrograph imposed at the inlet and considering different rheological index (n), several values of the Froude (F) and of the Kinematic Wave (K) numbers. The applicability conditions are expressed considering as indicators the mean values of the dimensionless error on the maximum flow depth and on the maximum discharge, ε_h^* and ε_q^*, respectively. Since positive errors lead to an overestimation of the maximum flow depth and flow rate, in the presented analysis the DWM is considered safely applicable for positive values of ε_h^* and ε_q^* and for negative values larger than -5%.

About the mean error on the maximum flow depth, present results indicate that it monotonically decreases with the wave duration, with an asymptotic minimum negative value $\varepsilon_{h,min}^*$ corresponding to quasi-steady conditions. Conversely, the mean error of the maximum flow discharge starting from a values at the lowest wave duration $\left(\varepsilon_{q,min}^*\right)$ achieves a maximum positive value and then it decreases tending asymptotically to zero for quasi-steady conditions. These observations suggest that the conditions $\varepsilon_{h,min}^* > -5\%$ and $\varepsilon_{q,min}^* > -5\%$ guarantees the applicability of the DWM, independently of the wave duration, in terms of maximum flow depth and discharge, respectively. Conversely when $\varepsilon_{h,min}^* < -5\%$, there exists an upper bound of the wave duration below which the DWM can be safely applied for predicting the flow depth. Similarly, when $\varepsilon_{q,min}^* < -5\%$ the DWM can be adopted for evaluating the maximum discharge when the wave duration is larger than a lower bound.

For a fixed rheology, the study of the $\varepsilon_{h,min}^*$ and $\varepsilon_{q,min}^*$ variability with respect to the governing dimensionless parameters F and K suggests that for a fixed F, the condition $\varepsilon_{h,min}^* > -5\%$ (resp. $\varepsilon_{q,min}^* > -5\%$) is satisfied when the kinematic wave number exceeds the threshold value $\overline{K}_h$ (respectively $\overline{K}_q$). Indeed, DWM can be safely applied independently of the hydrograph wave duration for the flow depth (resp. the flow rate) prediction whenever K is larger than $\overline{K}_h$ (resp. $\overline{K}_q$). The $\overline{K}_h$ and $\overline{K}_q$. values have been determined for several values of the (n, F) pair.

When the condition on K is not verified, i.e. $K < \overline{K}_h$ (respectively $K < \overline{K}_q$), further maps have been derived for evaluating the upper and lower bounds of wave duration for the safe application of the DWM in predicting the flow depth and the discharge, respectively.

The presented results clearly indicate that the rheology substantially affects the magnitude of the errors, reducing the applicability of DWM for shear-thinning fluids. Finally, the proposed methodology has been applied to two mud-flows occurred in 1999 in Southern Italy and involving fluids with pronounced shear-thinning behaviour. It has shown that even in these extreme conditions the applicability region of the DWM is still of technical interest.

Authors contributions

Conceptualization, C.D.C., M.I., T.M. and A.V.; software, C.D.C., M.I., A.V; data analysis, C.D.C., M.I. and A.V.; writing—review and editing, C.D.C., M.I., T.M. and A.V.; All authors have read and agreed to the published version of the manuscript.

Funding

Declaration of Competing Interest

The authors declare that they have no known competing financial interests or personal relationships that could have appeared to influence the work reported in this paper.

References

Ancey, C., Andreini, N., Epely-Chauvin, G., 2012. Viscoplastic dambreak waves: Review of simple computational approaches and comparison with experiments. Adv. Water Resour. 48, 79–91. https://doi.org/10.1016/j.advwatres.2012.03.015.

Arattano, M., Franzi, L., 2010. On the application of the kinematic model to simulate diffusive process of debris flows. Nat. Hazard Earth Syst. Sci. 10 (8), 1689–1695. https://doi.org/10.5194/nhess-10-1689-2010.

Aricò, C., Sinagra, M., Begnudelli, L., Tucciarelli, T., 2011. MAST-2D diffusive model for flood prediction on domains with triangular Delaunay unstructured meshes. Adv. Water Resour. 34 (11), 1427–1449. https://doi.org/10.1016/j.advwatres.2011.08.002.

Aricò, C., Nasello, C., 2018. Comparative analyses between the zero-inertia and fully dynamic models of the shallow water equations for unsteady overland flow propagation. Water 10 (1), 44. https://doi.org/10.3390/w10010044.

Armanini, A., Larcher, M., Nucci, E., Dumbser, M., 2014. Submerged granular channel flows driven by gravity. Adv. Water Resour. 63, 1–10. https://doi.org/10.1016/j.advwatres.2013.10.007.

Benavides-Solorio, J., MacDonald, L.H., 2005. Measurement and prediction of post-fire erosion at the hillslope scale, Colorado Front Range. Int. J. Wildland Fire 14 (4), 457–474. https://doi.org/10.1071/WF05042.

Bernard, M., Boreggio, M., Degetto, M., Gregoretti, C., 2019. Model-based approach for design and performance evaluation of works controlling stony debris flows with an application to a case study at Rovina di Cancia (Venetian Dolomites, Northeast Italy). Sci. Total Environ. 688, 1373–1388. https://doi.org/10.1016/j.scitotenv.2019.05.468.

Brown, R.A., Pasternack, G.B., 2014. Hydrologic and topographic variability modulate channel change in mountain rivers. J. Hydrol. 510, 551–564. https://doi.org/10.1016/j.jhydrol.2013.12.048.

Carotenuto, C., Merola, M.C., Álvarez-Romero, M., Coppola, E., Minale, M., 2015. Rheology of natural slurries involved in a rapid mudflow with different soil organic carbon content. Colloids Surf. A 466, 57–65. https://doi.org/10.1016/j.colsurfa.2014.10.037.

Cascini, L., Cuomo, S., De Santis, A. 2011. Numerical Modelling of the December 1999 Cervinara Flow-Like Mass Movements (Southern Italy). Italian Journal of Engineering Geology and Environment – Book. 5th International Conference on Debris-Flow Hazards Mitigation: Mechanics, Prediction and Assessment. 635–644. https://dx.doi.org/10.4408/IJEGE.2011-03.B-069.

Caviedes-Voullieme, D., Fernandez-Pato, J., Hinz, C., 2020. Performanc assessment of 2D Zero-Inertia and Shallow Water model for simulating rainfall-runoff processes. J. Hydrol. 584 https://doi.org/10.1016/j.jhydrol.2020.124663.

Chambon, G., Ghemmour, A., Naaim, M., 2014. Experimental investigation of viscoplastic free-surface flows in a steady uniform regime. J. Fluid Mech. 754, 332–364. https://doi.org/10.1017/jfm.2014.378.

Chanson, H., Jarny, S., Coussot, P., 2006. Dam break wave of thixotropic fluid. J. Hydraul. Eng. 132 (3), 280–293. https://doi.org/10.1061/(asce)0733-9429(2006)132:3(280).

Chen, J.C., Jan, C.D., Lee, M.S., 2008. Reliability analysis of design discharge for mountainous gully flow. J. Hydraulic Res. 46 (6), 835–838. https://doi.org/10.1080/00221686.2008.9521928.

Chiang, S.H., Chang, K.T., Mondini, A.C., Tsai, B.W., Chen, C.Y., 2012. Simulation of event-based landslides and debris flows at watershed level. Geomorphology 138, 306–318. https://doi.org/10.1016/j.geomorph.2011.09.016.

Ciervo, F., Papa, M.N., Medina, V., Bateman, A., 2015. Simulation of flash floods in ungauged basins using post-event surveys and numerical modelling. J Flood Risk Manage. 8 (4), 343–355. https://doi.org/10.1111/jfr3.12103.

Coussot, P., 1997. Mudflow Rheology and Dynamics. Balkema, Rotterdam.

Di, B.F., Chen, N.S., Cui, P., Li, Z.L., He, Y.P., Gao, Y.C., 2008. GIS-based risk analysis of debris flow: an application in Sichuan, southwest China. Int. J. Sedim. Res. 23 (2), 138–148. https://doi.org/10.1016/S1001-6279(08)60013-X.

Di Cristo, C., Iervolino, M., Vacca, A., 2013a. Waves dynamics in a linearized mud-flow shallow model. Appl. Math. Sci. 7, 377–393. https://doi.org/10.12988/ams.2013.13033.

Di Cristo, C., Iervolino, M., Vacca, A., 2013b. Gravity-Driven Flow of a Shear-Thinning Power– Law Fluid over a Permeable Plane. Appl. Math. Sci. 7 (33), 1623–1641. https://doi.org/10.12988/ams.2013.13150.

Di Cristo, C., Iervolino, M., Vacca, A., 2014a. Applicability of kinematic, diffusion and quasi-steady dynamic wave models to shallow mud flows. J. Hydrol. Eng. 19 (5), 956–965. https://doi.org/10.1061/(ASCE)HE.1943-5584.0000881.

Di Cristo, C., Iervolino, M., Vacca, A., 2014b. Simplified wave models applicability to shallow mud flows modeled as power-law fluids. J. Mountain Sci. 11 (6), 1454–1465. https://doi.org/10.1007/s11629-014-3065-6.

Di Cristo, C., Greco, M., Iervolino, M., Leopardi, A., Vacca, A., 2016. Two-dimensional two-phase depth-integrated model for transients over mobile bed. J. Hydraul. Eng. 142 (2), 04015043. https://doi.org/10.1061/(ASCE)HY.1943-7900.0001024.

Di Cristo C., Iervolino M., Vacca A. 2017. A strategy for passive control of natural roll-waves in power-law fluids through inlet boundary conditions. J. Appl. Fluid Mech., 10(2): 667–680. https://dx.doi.org/10.18869/acadpub.jafm.73.238.26945.

Di Cristo, C., Iervolino, M., Vacca, A., 2018a. Applicability of Kinematic and Diffusive models for mud-flows: a steady state analysis. J. Hydrol. 559, 585–595. https://doi.org/10.1016/j.jhydrol.2018.02.016.

Di Cristo, C., Iervolino, M., Vacca, A., 2018b. Wave propagation in linearized shallow flows of power-law fluids. Adv. Water Resour. 120, 35–49. https://doi.org/10.1016/j.advwatres.2017.06.022.

Di Cristo, C., Iervolino, M., Moramarco, T., Vacca, A., 2019. Applicability of Kinematic model for mud-flows: an unsteady analysis. J. Hydrol. 577, 123967 https://doi.org/10.1016/j.jhydrol.2019.123967.

Di Cristo, C., Greco, M., Iervolino, M., Vacca, A., 2020. Interaction of a dam-break wave with an obstacle over an erodible floodplain. J. Hydroinf. 22 (1), 5–19. https://doi.org/10.2166/hydro.2019.014.

Fent, I., Putti, M., Gregoretti, C., Lanzoni, S., 2018. Modeling shallow water flows on general terrains. Adv. Water Resour. 12, 316–332. https://doi.org/10.1016/j.advwatres.2017.12.017.

Fuchs S., Heiss K., Hübl J. 2007. Towards an empirical vulnerability function for use in debris flow risk assessment. Natural Hazards and Earth System Science, 7: 495–506. www.nat-hazards-earth-syst-sci.net/7/495/2007/.

Govindaraju, R.S., Jones, S.E., Kavvas, M.L., 1988a. On the diffusion wave model for overland flow: Solution for steep slopes. Water Resour. Res. 24 (5), 734–744. https://doi.org/10.1029/WR024i005p00734.

Govindaraju, R.S., Jones, S.E., Kavvas, M.L., 1988b. On the diffusion wave model for overland flow: Steady state analysis. Water Resour. Res. 24 (5), 745–754. https://doi.org/10.1029/WR024i005p00745.

Greco, M., Di Cristo, C., Iervolino, M., Vacca, A., 2019. Numerical simulation of mud-flows impacting structures. J. Mountain Sci. 16, 364–382. https://doi.org/10.1007/s11629-018-5279-5.

Gregoretti, C., Degetto, M., Boreggio, M., 2016. GIS-based cell model for simulating debris flow runout on a fan. J. Hydrol. 534, 326–340. https://doi.org/10.1016/j.jhydrol.2015.12.054.

Gregoretti, C., Stancanelli, L.M., Bernard, M., Boreggio, M., Degetto, M., Lanzoni, S., 2019. Relevance of erosion process when modelling mine in-channel gravel debris flows for efficient hazard assessment. J. Hydrol. 568, 575–591. https://doi.org/10.1016/j.jhydrol.2018.10.001.

Hewitt, D.R., Balmforth, N.J., 2013. Thixotropic gravity currents. J. Fluid Mech. 727, 56–82. https://doi.org/10.1017/jfm.2013.235.

Huang, X., Garcia, M.H., 1998. A Herschel-Bulkley model for mud flow down a slope. J. Fluid Mech. 374, 305–333. https://doi.org/10.1017/S0022112098002845.

Hurlimann, M., Copons, R., Altimir, J., 2006. Detailed debris flow hazard assessment in Andorra: a multidisciplinary approach. Geomorphology 78, 359–372. https://doi.org/10.1016/S0098-3004(00)00124-2.

Hutter, K., Svendsen, B., Rickenmann, D., 1994. Debris flow modeling: A review. Continuum Mech. Thermodyn. 8 (1), 1–35.

Hwang, C.C., Chen, J.L., Wang, J.S., Lin, J.S., 1994. Linear stability of power law liquid film flowing down an inclined plane. J. Physic D Appl. Phys. 27, 2297–2301. https://doi.org/10.1088/0022-3727/27/11/008.

Imran, J., Harff, P., Parker, G., 2001. A numerical model of submarine debris flows with graphical user interface. Comput. Geosci. 27 (6), 717–729.

Iverson, R.M., 1997. The physics of debris flows. Rev. Geophys. 35 (3), 245–296. https://doi.org/10.1029/97RG00426.

Iverson, R.M., Denlinger, R.P., 2001. Flow of variably fluidized granular masses across three-dimensional terrain: Coulomb mixture theory. J. Geophys. Res. Solid Earth 106 (B1), 537–552. https://doi.org/10.1029/2000JB900329.

Iverson, R.M. 2003. The debris-flow rheology myth. Proceedings of International Conference on Debris-Flow Hazards Mitigation: Mechanics, Prediction, and Assessment, Davos: 303–314.

Iverson, R.M., George, D.L., 2014. A depth-averaged debris-flow model that includes the effect of evolving dilatancy. I Physical basis. Proc. R. Soc. A Math. Phys. Eng. Sci. 470, 1–31. https://doi.org/10.1098/rspa.2013.0819.

Li, J., Cao, Z.X., Hu, K.H., et al., 2018a. A depth-averaged two-phase model for debris flows over fixed beds. Int. J. Sedim. Res. 33 (4), 462–477. https://doi.org/10.1016/j.ijsrc.2017.06.003.

Li, J., Cao, Z.X., Hu, K.H., et al., 2018b. A depth-averaged two-phase model for debris flows over erodible beds. Earth Surface Process. Landform 43 (4), 817–839. https://doi.org/10.1002/esp.4283.

Liu, K.F., Mei, C.C., 1989. Slow spreading of a sheet of Bingham fluid on an inclined plane. J. Fluid Mech. 207, 505–529. https://doi.org/10.1017/S0022112089002685.

Longo, S., Di Federico, V., Chiapponi, L., 2015. Non-Newtonian power-law gravity currents propagating in confining boundaries. Environ. Fluid Mech. 15, 515–535. https://doi.org/10.1007/s10652-014-9369-9.

Martins, R., Leandro, J., Chen, A.S., Djordjević, S. 2017. A comparison of three dual drainage models: shallow water vs local inertial vs diffusive wave. J. Hydroinf., 19 (3):331–348, doi:hydro.2017.075.full.pdf.

Moramarco, T., Pandolfo, C., Singh, V.P., 2008a. Accuracy of kinematic wave and diffusion wave approximations for flood routing. I: Steady analysis. J. Hydrol. Eng. 13 (11), 1078–1088. https://doi.org/10.1061/(ASCE)1084-0699(2008)13:11(1078).

Moramarco, T., Pandolfo, C., Singh, V.P., 2008b. Accuracy of kinematic wave approximations for flood routing. II: Unsteady analysis. J. Hydrol. Eng. 13 (11), 1089–1096. https://doi.org/10.1061/(ASCE)1084-0699(2008)13:11(1089).

Nash, J.E., Sutcliffe, J.V., 1970. River flow forecasting through conceptual models. Part I: A discussion of principles. J. Hydrol. 10 (3), 282–290. https://doi.org/10.1016/0022-1694(70)90255-6.

Ng, C., Mei, C.C., 1994. Roll waves on a shallow layer of mud modeled as a power-law fluid. J. Fluid Mech. 263, 151–184. https://doi.org/10.1017/S0022112094004064.

O'Brien, J.S., Julien, P.Y., Fullerton, W.T., 1993. Two-dimensional water flood and mudflow simulation. J. Hydraul. Eng. 119 (2), 244–261. https://doi.org/10.1061/(ASCE)0733-9429(1993)119:2(244).

Ovarlez, G., Mahaut, G., Bertrand, F., Chateau, X., 2011. Flows and heterogeneities with a vane tool: magnetic resonance imaging measurements. J. Rheol. 55 (2), 197–223. https://doi.org/10.1122/1.3526349.

Pascal, H., 1991. Gravity flow of a non-Newtonian fluid sheet on an inclined plane. Int. J. Eng. Sci. 29 (10), 1307–1313. https://doi.org/10.1016/0020-7225(91)90035-2.

Perazzo, C.A., Gratton, J., 2004. Steady and traveling flows of a power–law liquid over an incline. J. Nonnewton. Fluid Mech. 118, 57–64. https://doi.org/10.1016/j.jnnfm.2004.02.003.

Pitman, E.B., Le, L., 2005. A two-fluid model for avalanche and debris flows. Philosophical Transactions of the Royal Society A. Math. Phys. Eng. Sci. 363, 1573–1601. https://doi.org/10.1098/rsta.2005.1596.

Prestinizi, P., 2008. Suitability of the diffusive model for dam break simulation: application to CADAM experiment. J. Hydrol. 361 (1–2), 172–185. https://doi.org/10.1016/j.jhydrol.2008.07.050.

Rengers, F.K., McGuire, L.A., Kean, J.W., Staley, D.M., Hobley, D.E.J., 2016. Model simulations of flood and debris flow timing in steep catchments after wildfire. Water Resour. Res. 52 (8), 6041–6061. https://doi.org/10.1002/2015WR018176.

Rosatti, G., Begnudelli, L., 2013. Two dimensional simulations of debris flows over mobile beds: enhancing the TRENT2D model by using a well-balanced generalized Roe-type solver. Comput. Fluids. 71, 179–185. https://doi.org/10.1016/j.compfluid2012.10.006.

Stoof, C.R., Vervoort, R., Iwema, J., Elsen, E., Ferreira, A., Ritsema, C., 2012. Hydrological response of a small catchment burned by experimental fire. Hydrol. Earth Syst. Sci. 16 (2), 267–328. https://doi.org/10.5194/hess-16-267-2012.

Takahashi, T. 1991. Debris Flows, IAHR Monograph, Balkema, Rotterdam.

Thiene, M., Shaw, W.D., Scarpa, R., 2017. Perceived risks of mountain landslides in Italy: stated choices for subjective risk reductions. Landslides 14 (3), 1077–1089. https://doi.org/10.1007/s10346-016-0741-3.

Tsai, C.W., 2003. Applicability of kinematic, noninertia, and quasisteady dynamic wave models to unsteady flow routing. J. Hydraul. Eng. 129 (8), 613–627. https://doi.org/10.1061/(ASCE)0733-9429(2003)129:8(613).

VanDine, D.F., 1985. Debris flow and debris torrents in the Southern Canadian Cordillera. Can. Geotech. J. 22 (1), 44–68. https://doi.org/10.1139/t85-006.

Xia, C.C., Li, J., Cao, Z.X., et al., 2018. A quasi single-phase model for debris flows and its comparison with a two-phase model. J. Mountain Sci. 15 (5), 1071–1089. https://doi.org/10.1007/s11629-018-4886-5.

Zucco, G., Tayfur, G., Moramarco, T., 2015. Reverse Flood Routing in Natural Channels using Genetic Algorithm. Water Resour. Manag. 29 (12), 4241–4267. https://doi.org/10.1007/s11269-015-1058-z.

Zhang, X., Bai, Y., Ng, C.O. 2010. Rheological Properties of Some Marine Muds Dredged from China Coasts. In: Proceedings of the 28th International Offshore and Polar Engineering Conference, Beijing, China: 455–461.

Zheng, H., Huang, E., Luo, M., 2020. Applicability of kinematic wave model for flood routing under unsteady inflow. Water 12, 2528. https://doi.org/10.3390/w12092528.